Electronic Supplementary Information

Immobilization of carbonyl rhenium tripods on the surface of trinickle-substituted Dawson-type polyoxotungsate

Jiage Jia, Pengtao Ma, Panpan Zhang, Dongdi Zhang, Chao Zhang, Jingyang Niu* and Jingping Wang*

Henan Key Laboratory of Polyoxometalate Chemistry,
Institute of Molecular and Crystal Engineering,
College of Chemistry and Chemical Engineering,
Henan University, Kaifeng 475004, Henan, China,
E-mail: jyniu@henu.edu.cn; Fax: (+86)371-23886876.

CONTENTS

Section S1: A summary of the isolated monomeric Keggin or Dawson type Ni-substituted POT

Table S1 A summary of the isolated monomeric Keggin or Dawson type Ni-substituted POT

Type	monomeric Ni-substituted POT	Syntheses method	Ref
Keggin	$\{Ni_3(H_2O)_3(PW_{10}O_{39})H_2O\}$	In conventional aqueous solution,refluxed	1
	$\{H_2Ni_4PW_9O_{34}(OH)_3(H_2O)_6\}$	In conventional aqueou solution	2
	$\{Ni_6(OH)_3(H_2O)_6(L)_3(B\text{-}\alpha\text{-}XW_9O_{34})\}$ (X=P, Si, Ge; L=en or dap)	Hydrothermal method	3
	$\{[Ni(H_2O)(en)_2][WO_4][Ni_6(OH)_3(H_2O)_2(en)_3(Im)_2](B\text{-}PW_9O_{34})\}$	Hydrothermal method	4
	$\{(A\text{-}a\text{-}SiW_9O_{34})KNi_4(OH)_3((SC_4H_3)CH_2COO)_3\}$	In conventional aqueou solution	5
Dawson	$\{Ni_3(OH)_3(H_2O)_3P_2W_{16}O_{59}\}$	In conventional aqueou solution	6
	$\{P_2W_{15}O_{56}(W_{0.5}Ni_{3.5})(OH)_6(H_2O)_3\}$	In conventional aqueou solution	7
	$\{Ni_6(\mu_3\text{-}OH)_3(H_2O)_3(Y)_3H_3(\alpha\text{-}P_2W_{15}O_{56})\}$ (Y = dien, en)	Hydrothermal method	8
	$\{Ni_6(Y)_3(H_2O)_6(\mu_3\text{-}OH)_3(H_3P_2W_{15}O_{56})\}$ (Y = en, enMe)	Hydrothermal method	9
	$\{Ni_6(H_2O)_6Y(\mu_3\text{-}OH)_3(H_3P_2W_{15}O_{56})$ (Y = en, $(dap)_2(en)$)	Hydrothermal method	10

Section S2: Materials and instrumentation

$Na_{12}[(\alpha\text{-}P_2W_{15}O_{56})]\cdot 24H_2O$ was synthesized as previously described.[11] All other chemicals were reagent grade and used as purchased without purification. FT-IR spectra were measured on a Bruker VERTEX 70 IR spectrometer using KBr pellets in the range of 4000–500 cm^{-1}. Elemental analyses of C, H, and N were performed with a PerkinElmer 2400−II CHNS/O analyzer. Inductively coupled plasma (ICP) spectra were obtained on a Perkin-Elmer Optima 2000 ICP-OES spectrometer. Energy-dispersive X-ray spectroscopy (EDX) measurement was performed on a JSM-7610F scanning electron microscope using OXFORD x-act EDX. X-ray powder diffraction (XRD) spectral data were recorded on a Bruker AXS D8 Advance diffractometer with Cu Kα radiation in the angular range $2\theta = 5–45°$ at 293 K. UV spectra were obtained with a U-4100 spectrometer at room temperature. All electrochemical measurements were performed at room temperature in a standard three-electrode cell connected to a CGI660E B15375 microcomputer-based electrochemical system. A freshly cleaned glassy carbon disk electrode (3 mm diameter) was used as a working electrode, a platinum wire served as the counter electrode and SCE as the reference electrode. Magnetic susceptibility measurements were carried out with a

Quantum Design SQUID (MPMS3 and PPMS-9) magnetometer in the temperature range of 1.8–300 K. The susceptibility data were corrected from the diamagnetic contributions as deduced by using Pascal's constant tables.

Section S3: X-ray crystallography

Suitable single crystal of **1**, was selected from their respective mother liquor and airproofed in a glass tube. X-ray diffraction intensity data were recorded on a Bruker APEX-II CCD diffractometer with graphite-monochromated Mo Kα radiation (λ = 0.71073 Å). Routine Lorentz and polarization corrections were applied. The absorption correction was based on multiple and symmetry equivalent reflections in the data set using the SADABS program. The structure was solved by direct methods and refined using full-matrix least squares on F^2. The crystal was kept at 296 (2) K during data collection. Using Olex2,[12] the structure was solved with the SHELXS-97 structure solution program using Direct Methods and refined with the SHELXL-14 refinement package using Least Squares minimisation.[13, 14] The W, Ni, Re and P heavy atoms were refined anisotropically; all the O and C atoms were refined isotropically. No hydrogen atoms associated with the partial water molecules were located from the difference Fourier map. The remaining lattice water molecules were determined by TGA results. A summary of the crystal data and structure refinements parameters is listed in Table S2. CCDC-1567167 for **1** can be obtained free of charge from The Cambridge Crystallographic Data Centre.

Table S2. Crystal data and structure refinement parameters for compound **1**

Empirical formula	$C_9H_{46}O_{91}P_2Re_3W_{15}Ni_3$
Formula weight	5164.88
Temperature	296.15
Crystal system	monoclinic
space group	$P2_1/m$
a/[Å]	14.5956(7)
b/[Å]	22.3215(11)
c/[Å]	14.8504(7))
β[o]	91.1100(10)
Z	2
Volume/[Å3]	4837.3(4)
Calculated density/[g·cm^{-3}]	3.546
μ/[mm-1]	22.199
F(000)	4554
Crystal size	0.36 × 0.15 × 0.13
Theta range for data collection	3.65 to 50.198
Limiting indices	-17<=h<=17, -26<=k<=26, -17<=l<=15
Reflections collected	25112
Independent reflections	8806 [R_{int} = 0.0463] R_{sigma} = 0.0549]
Data / restraints / parameters	8806/ 6 /334
Goodness-of-fit on F^2	1.016
Final R indices [I >2σ(I)]	R_1 = 0.0406, wR_2 = 0.0994
R indices (all data)	R_1 = 0.0588, wR_2 = 0.1100

Largest diff. peak and hole/[e·Å^{-3}]	2.94, -1.57

Table S3 Bond valence sum calculations of W、P、Ni and O atoms of compound **1**

Atom	VBS	Atom	VBS	Atom	VBS
W1	6.273	O7	1.827	O25	1.988
W2	6.107	O8	2.015	O26	2.016
W3	6.148	O9	2.097	O27	1.739
W4	6.237	O10	2.016	O28	1.685
W5	6.250	O11	1.970	O29	1.768
W6	6.263	O12	1.960	O30	1.757
W7	6.133	O13	1.267	O31	1.675
W8	6.235	O14	1.779	O32	1.911
P1	4.846	O15	1.989	O33	1.687
P2	5.024	O16	2.032	O34	2.011
Ni1	1.973	O17	1.906	O35	2.123
Ni2	1.827	O18	1.362	O36	0.332
O1	1.869	O19	1.730	O37	0.204
O2	2.152	O20	1.853	O38	1.960
O3	2.064	O21	2.109	O39	1.708
O4	2.191	O22	2.157	O40	1.748
O5	2.090	O23	2.117	O41	1.838
O6	2.173	O24	2.009	O42	1.770

Table S4 Part bond length (Å) and bond angle (°) of compound **1**

Bonds	Length/Å	Bonds	Angle/°
Ni1-O4	2.052(9)	Ni1-O12-Ni2	94.2(4)
Ni1-O41	2.052(9)	Ni1-O12-Ni2A	94.2(4)
Ni1-O12	2.110(12)	Ni2-O12-Ni2A	94.4(5)
Ni1-O13	2.060(9)	Ni2-O13-Ni1	99.1(4)
Ni1-O36	2.061(16)	Ni2-O18-Ni2A	102.1(6)
Ni2-O2	2.064(9)	Ni2-O2-Re1	100.6(4)
Ni2-O6	2.087(9)	Ni1-O4-Re1	100.3(4)
Ni2-O12	2.148(8)	Ni2-O6-Re2	99.1(4)
Ni2-O13	2.037(9)	Ni1-O13-Re1	99.7(4)
Ni2-O18	2.028(8)	Ni2-O13-Re1	102.2(4)
Ni2-O37	2.241(8)	Ni2A-O18-Re2	102.9(4)
Re1-O2	2.194(9)	Ni2-O18-Re2	102.9(4)
Re1-O4	2.163(9)	O39-C1-Re1	177.3(14)
Re1-O13	2.172(8)	O38-C2-Re1	174.2(14)
Re1-C1	1.857(16)	O40-C3-Re1	178.0(16)
Re1-C2	1.878(16)	O42-C4-Re2	178.3(18)
Re1-C3	1.858(17)	O41-C5-Re2	179(2)

Re2-O6	2.197(9)	C1-Re1-O13	171.9(5)
Re2A-O6	2.197(9)	C2-Re1-O2	170.9(5)
Re2-O18	2.139(13)	C3-Re1-O4	174.0(6)
Re2-C4	1.844(19)	C4-Re2-O6	173.4(6)
Re2A-C4	1.844(19)	C4A-Re2-O61	173.4(6)
Re2-C5	1.86(3)	C5-Re2-O18	173.5(8)

Section S4: Synthesis of compound **1**

Synthesis of Compound 1 (Re-Ni). A sample of $Na_{12}[P_2W_{15}O_{56}]\cdot 18H_2O$ (0.22 g, 0.05 mmol), $Ni(OAc)_2\cdot 4H_2O$ (0.0373 g, 0.15 mmol), LiOAc (0.02 g) were dissolved in the 12 mL H_2O. After vigorously stirring about 10 min at the room temperature, the pH value of the solution was about 6.00 and the mixture solution became clear green from muddy. Then, $Re(CO)_5Cl$ (0.054 g, 3 mL) solution refluxed in 3 mL CH_3CN in the dark for 0.5 h was added into the mixture. The resulting solution was continuously stirred about 1 h at 80 °C and became clear wine red solution. Finally, NH_4Cl (0.1 g) was added the solution and stirred at room temperature about 10 min, then cooled and filtrated. After slow evaporation at the room temperature in the dark, the filtrate produced red black stick crystals after three weeks. Yield: ca. 25.78 % (based on P_2W_{15}). Anal. calcd (found %) for: C 2.06 (2.08), H 1.25 (1.28), N 1.34 (1.41), P 1.18 (1.20), Ni 3.36 (3.39), Re 10.65 (10.95), W 52.58 (52.72), Na 0.43 (0.46). IR (KBr, cm^{-1}): 3468 (m), 3136(m), 2018 (vs), 1890 (vs), 1614 (s), 1402(vs), 1086 (s), 1052 (w), 1016 (w), 955 (w), 938 (s), 908 (s), 768 (vs), 699 (s), 688 (w), 626 (w), 512 (w).

Section S5: XRD patterns of compound **1**

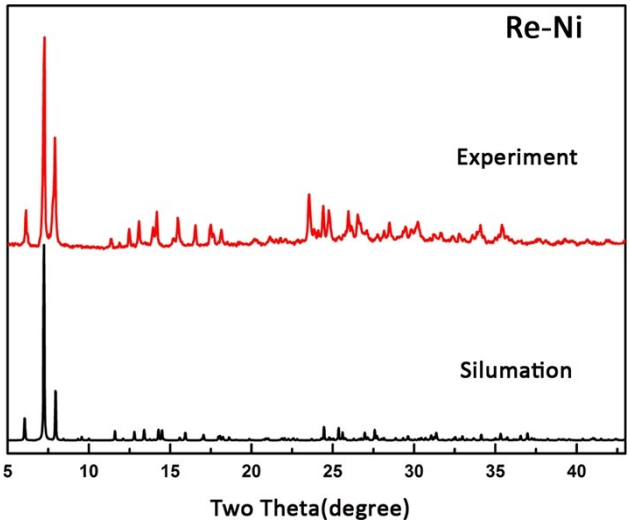

Fig.S1. Comparison of the simulated and experimental XRD patterns of **1**

Section S6: TGA analysis

The thermal stability of **1** has been investigated under nitrogen atmospheres with slow heating rate of 5 °C/min from 25 to 700 °C by thermogravimetric analysis (TGA) (Figure S2). The TGA curve shows two steps of weight loss at the range of 25–700 °C. The first weight loss is 8.9 % (calcd 8.66 %) from 25 to 300 °C, assigned to the release of 18 lattice water molecules and 5 NH_4^+ cations (in the form of NH_3 and water molecules). The second weight loss is 9.48 % (calcd 9.10 %) at the range of 300–800 °C, which can be ascribed to the removal of 3 coordinated water molecules, 3 hydroxy groups (in the form of 1.5 constitution water molecules) and 3 CO molecules (in the form of CO_2 molecules).[15]

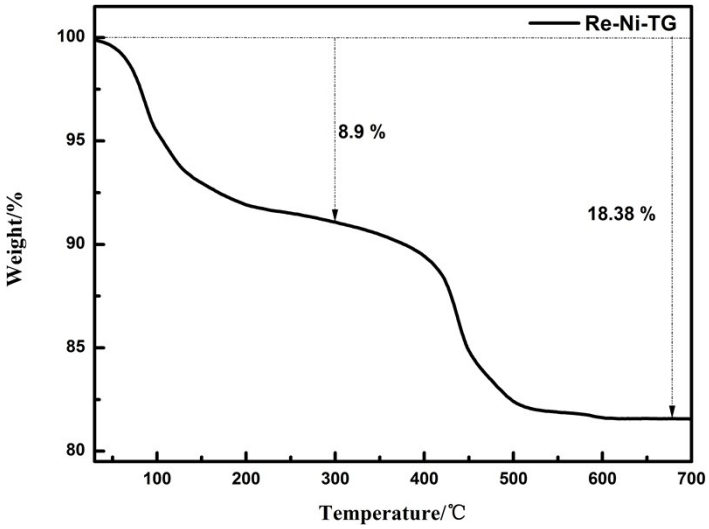

Fig.S2.TGA curve of **1**

Section S7: EDX analysis

We used EDX to characterize supplementary the composition of the title compound. According to the EDX spectrum, Ni and Re were detected with approximate ratio of Ni : Re found to be 1.05 : 1 and Ni and W were detected with approximate ratio of Ni : W found to be 4.9 : 1. This result has been checked using multiple samples to reduce the error in the value. However, as we know, the EDX measurements have about 8 % error estimated comparison with others POMs literatures. Therefore, using both the structural data and analysis by the EDX, ICP, TGA, charge balance arguments we are able to estimate the formula of the title compound. Using this approach we can give the formula of **1** is $Na(NH_4)_5[P_2W_{15}O_{56}Ni_3(H_2O)_3(OH)_3(Re(CO)_3)_3]\cdot 18H_2O$.

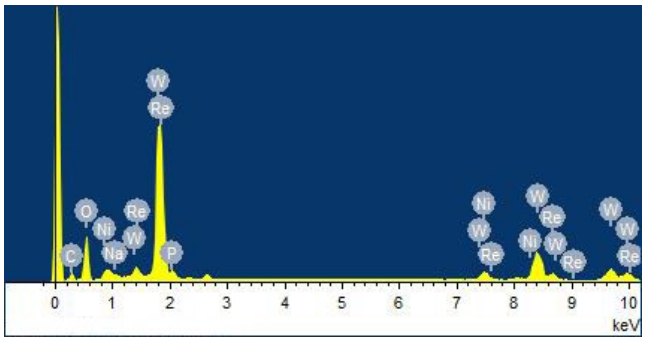

Fig. S3. EDX spectrum of single crystal of **1**

Section S8: IR spectra of **1** and **$[P_2W_{15}O_{56}]^{12-}$**

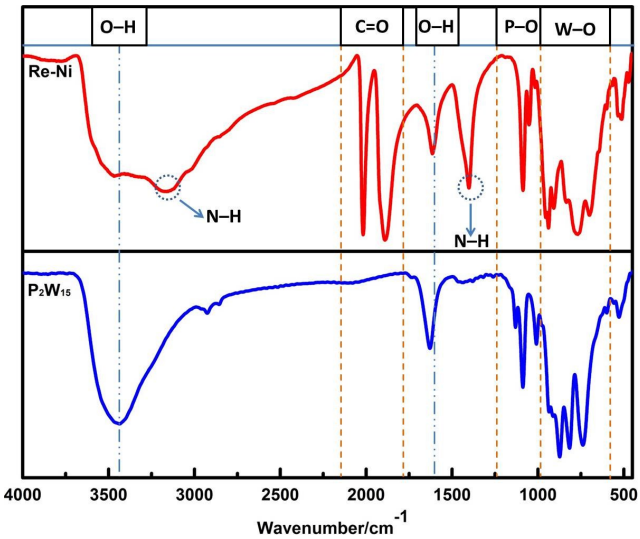

Fig. S4. IR spectra (KBr pellets) of **1** and $[P_2W_{15}O_{56}]^{12-}$

Section S9: Packing arrangement of polyanions of **1**

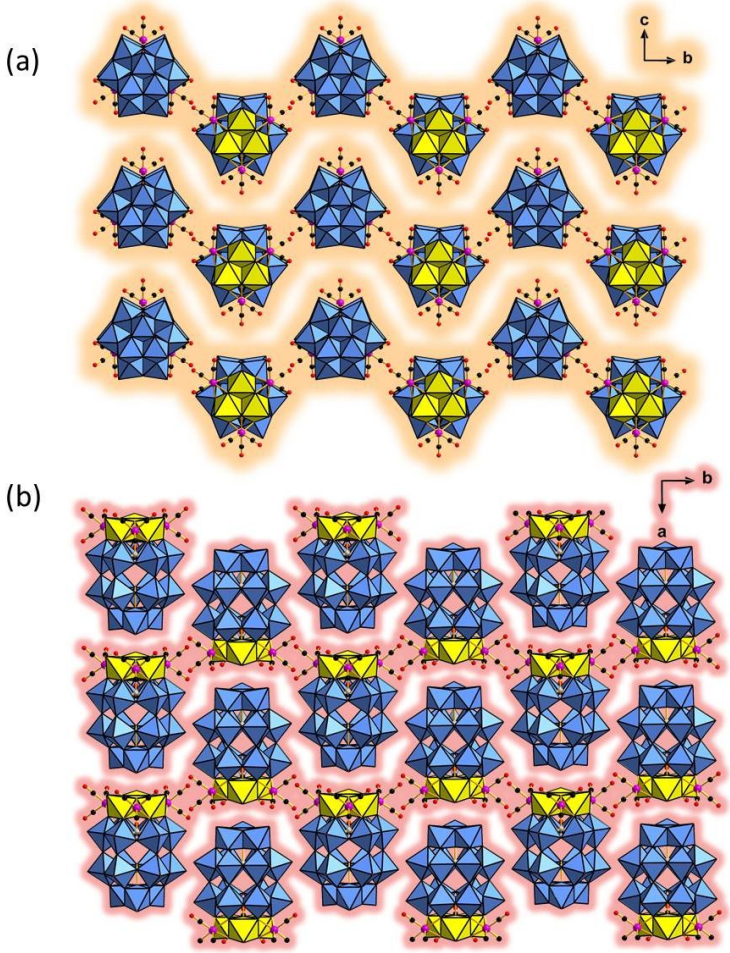

Fig. S5 Packing arrangement of polyanions of **1** along the a/c-axis

Section S10: The UV-vis spectra of **1**

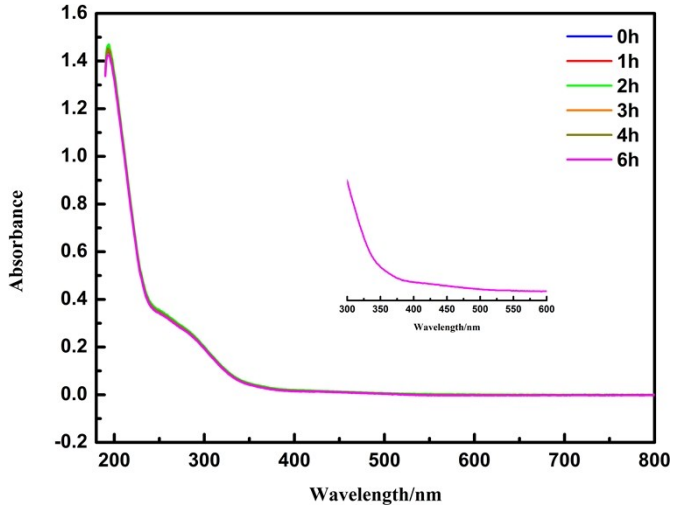

Fig.S6 The UV-vis spectra of **1** in the low concentrated solution with the time range (2.0×10^{-6} mol·L^{-1})

Section S11: The CV of **1**

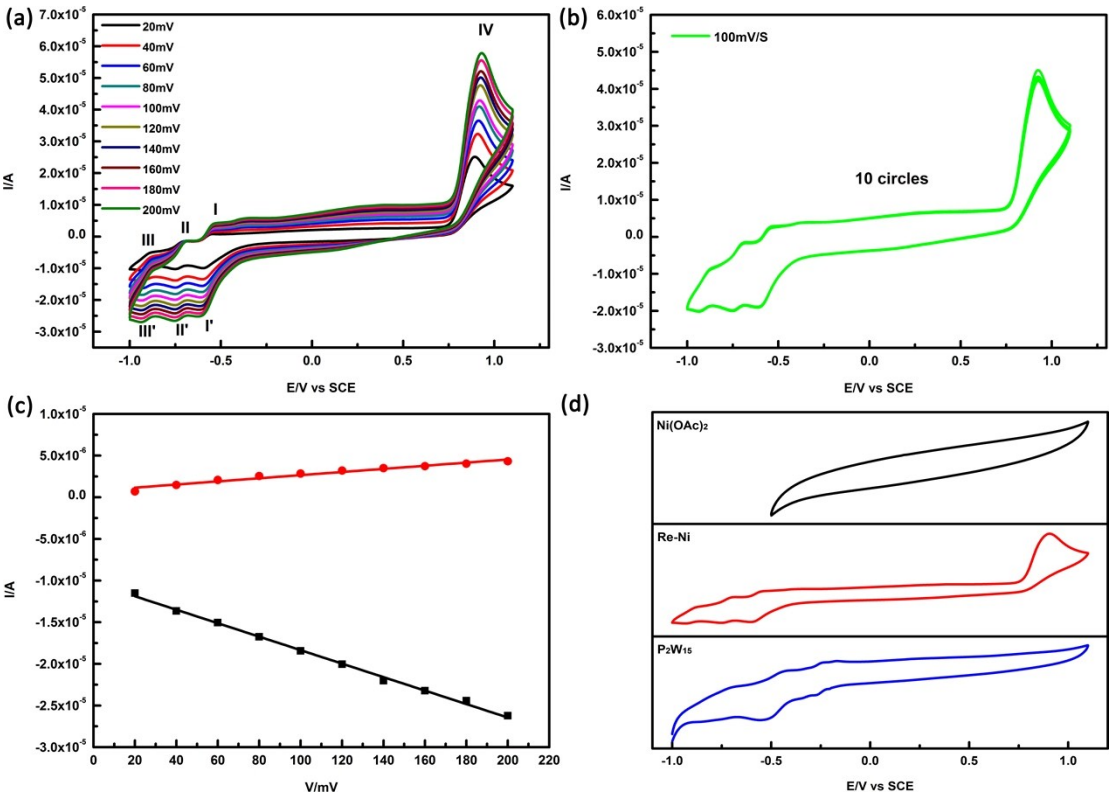

Fig. S7 (a) CV of **1** at diferent scan rates; (b) 10 circles of CV of **1** at 100 mV s^{-1}; (c) the variation of the peak current intensity for the redox pair of I/I' is proportional to the scan rates from 20 to 200 mV·s^{-1}; (d) the comparison of CV of **1**, $Ni(OAc)_2\cdot4H_2O$ and P_2W_{15}.·Conditions: 0.2 M Na_2SO_4–H_2SO_4 (pH = 4.00), c = 2.0×10^{-4} mol·L^{-1}.

Table S5 Comparison of voltammetric data for the W centers redox of compound **1** and $\mathbf{P_2W_{15}}$.

	I/I'		II/II'		III/III'	
	1	P_2W_{15}	**1**	P_2W_{15}	**1**	P_2W_{15}
E_{pa}/V	-0.54	-0.22	-0.69	-0.45	-0.88	-0.70
E_{pc}/V	-0.61	-0.28	-0.75	-0.54	-0.94	-0.76
$E_{1/2}$/V	-0.58	-0.25	-0.72	-0.50	-0.91	-0.73
ΔE_p/mV	70	60	60	90	60	60

Section S12: The field dependence of the magnetization of **1**

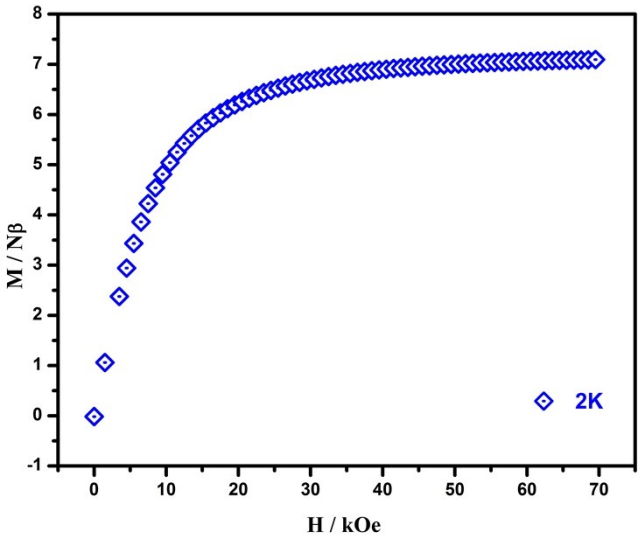

Fig. S8 The field dependence of the magnetization of **1** at 2 K

Section S13: The UV-vis diffuse reflectance spectra (DRS) of the compound **1**.

The UV-vis diffuse reflectance spectra (DRS) of the compound 1 were investigated and show three peaks. The band below 300 nm is attributed to the O(2p)→W(5d) transition. The band at 350 nm is assigned to the ligand-to-metal charge transfer (LMCT) band. The broad absorptions of **1** in the visible region is due to MPCT from the Re centers to POM ligands, which is consistent with the previous studies by Hill's group.[16] What's more, compared with the raw material $Re(CO)_5Cl$, we can see that the obviously red shift was present in the spectra, which further demonstrates the charge transition from Re centers to the POM ligands.

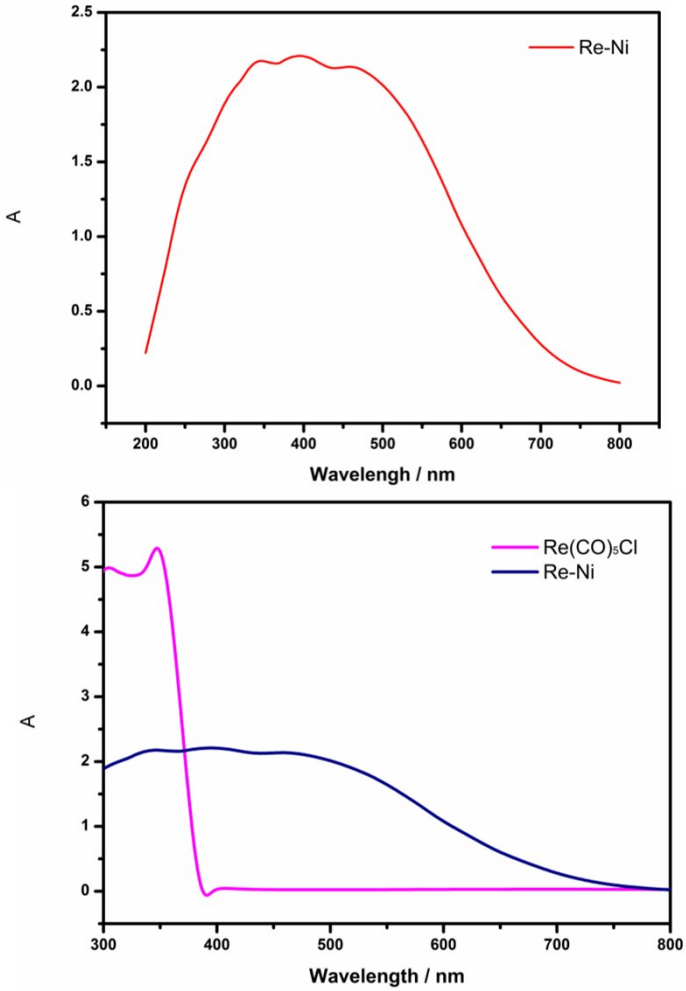

Fig. S9 The UV-vis diffuse reflectance spectra (DRS) of the compound **1** (a);
Compared with the raw material $Re(CO)_5Cl$ (b)

Section S14: References

1. J. M. Clemente-Juan, E. Coronado, J. R.Galán-Mascarós, and C. J. Gómez-García, *Inorg. Chem.*, 1999, **38**, 55-63.
2. U. Kortz, A. Teze, and G. Hervé, *Inorg. Chem.*, 1999, **38**, 2038–2042.

3. (a) S. T. Zheng, D. Q.Yuan, H. P. Jia, J. Zhang, and G. Y. Yang, *Chem. Commun.*, 2007 (18), 1858–1860; (b) J. W. Zhao, J. Zhang, Y. Song, S. T.Zheng, and G. Y. Yang, *Eur. J. Inorg. Chem.*, 2008, **2008**, 3809–3819.
4. J. W. Liu, Y. C. Liu, H. He, B. F. Yang, and G. Y. Yang, *Inorg. Chem. Commun.*, 2015, **53**, 60–63.
5. G. Rousseau, O. Oms, A. Dolbecq, J. Marrot, and P. Mialane, *Inorg. Chem.*,2011, **50**, 7376–7378.
6. W. W. Guo, H. Lv, J. Bacsa, Y. Z. Gao, J. S. Lee, and C. L. Hill, *Inorg. Chem.*, 2016, **55**, 461–466.
7. R. Wan, Y. Wang, M. Han, P. Ma, J. Niu and J. Wang, Inorg. *Chem. Commun.*, 2016, **68**, 72–75.
8. Y.-C. Liu, C.-H. Fu, S.-T. Zheng, J.-W. Zhao and G.-Y. Yang, *Dalton Trans.*, 2013, **42**, 16676–16679.
9. X.-X. Li, W.-H. Fang, J.-W. Zhao and G.-Y. Yang, *Chem. - Eur. J.*, 2014, **20**, 17324–17332.
10. X. Wang, S. Liu, Y. Liu, D. He, N. Li, J. Miao, Y. Ji and G. Yang, *Inorg. Chem.*, 2014, **5**3, 13130–13135.
11. R. Contant, W. G. Klemperer, O. Yaghi, *Inorg. Synth.,* 2007, **27**, 104–111.
12. O. V. Dolomanov, L. J. Bourhis, R. J.Gildea, J. A. K Howard, *J. Appl. Crystallogr.,* 2009, **42**, 339–341.
13. G. M. Sheldrick, *Acta Crystallogr. A.* 2008, **64**, 112–122.
14. G. M. Sheldrick, *Acta Crystallogr. Sect. C Struct. Chem.* **2015**, 71 (1), 3–8.
15. K. Nishiki, H. Ota, S. Ogo, T. Sano and M. Sadakane, *Eur. J. Inorg. Chem.*, 2015, **2015**, 2714–2723.
16. (a) C. Zhao, C. S. Kambara, Y. Yang, A. L. Kaledin, D. G. Musaev, T. Q. Lian and C. L. Hill, *Inorg. Chem.,* 2013, **52**, 671; (b) C. Zhao, Z. Huang, W. Rodr´ıguez-C´ ordoba, C. S. Kambara, K. P. O'Halloran, K. I. Hardcastle, D. G. Musaev, T. Lian and C. L. Hill, *J. Am. Chem. Soc.*, 2011, **133**, 20134;